Three-Antenna Two-Dimensional Imaging Correlation Radiometer: Concept and Preliminary Results

A. Camps, A. Sumpsi
Dept. of Signal Theory and Communications, Universitat Politècnica de Catalunya
Campus Nord, D4-016, E-08034 Barcelona, Spain
Tel. +34+934016085, Fax. +34+934017232, e-mail: camps@tsc.upc.es

***Abstract*— This paper presents the concept and preliminary experimental results of a two-dimensional imaging correlation radiometer formed by three antennas located at the vertices of an equilateral triangle. This radiometer concept is based on the Doppler-radiometer described in [1]. Due to the limited data record, in the experimental results presented, Doppler focusing was not possible, and only delay focusing was used. The radiometer antennas form very long baselines and, since the transit time to travel to the antenna positions is larger than the correlation time, signal decorrelates. The instrumental delays inserted before the computation of the signals' cross-correlations are then used to focus a particular direction, and correlating at different time lags an image is formed.**

I. BASIC PRINCIPLES The antenna array configuration is defined by the antenna positions: $R_1=(0,0)$, $R_2=(D_1,0)$, $R_3=(D_1/2,D_2)$.

Three baselines, named 1-2, 2-3 and 3-1, can be formed from the corresponding antenna pairs:

$$(u_{12},v_{12})=(R_2-R_1)/\lambda_0=(D_1,0)/\lambda_0 \triangleq (u,0),$$
$$(u_{23},v_{23})=(R_3-R_2)/\lambda_0=(-D_1/2,\ D_2)/\lambda_0 \triangleq (-u/2,\ v),$$
$$(u_{31},v_{31})=(R_1-R_3)/\lambda_0=(D_1/2,-D_2)/\lambda_0 \triangleq (\ u/2,-v). \quad (1)$$

where $\lambda_0=c/f_0$ is the electromagnetic wavelength at the center frequency f_0.

System's output $V_{123}(\tau_2,\tau_3)$ is formed by the intensity correlation of the signals $b_1(t-\tau_1)$, $b_2(t-\tau_2)$ and $b_3(t-\tau_3)$ collected by the three antennas, delayed with instrumental delays $\tau_1=0$, $\tau_2=u\xi/f_0$ and $\tau_3=(u\xi/2+v\eta)/f_0$ are inserted to focus the signals coming from the direction $(\xi,\eta)=(\sin\theta\cos\phi,\sin\theta\sin\phi)$:

$$V_{123}(\tau_2,\tau_3)= \overline{(b_1(t)b_1^*(t)-I_1)(b_2(t-\tau_2)b_2^*(t-\tau_2)-I_2)(b_3(t-\tau_3)b_3^*(t-\tau_3)-I_3)}. \quad (2)$$

where $I_n=\overline{b_n(t)b_n^*(t)}=\overline{|b_n(t)|^2}$ is the power of $b_n(t)$. Expanding eqn. (2) using of the circular joint Gaussian random variables Theorem [Goodman, 1985, p. 44], and assuming that $I_1=I_2=I_3$, eqn. 2 reduces to:

$$V_{123}(\tau_2,\tau_3)=2\,\mathrm{Re}[V_{12}V_{23}V_{31}], \quad (3)$$

where $V_{lm}=\overline{b_l(t-\tau_l)b_m^*(t-\tau_m)}$ is the amplitude complex cross-correlation between the signals collected by the element pair *l* and *m*, with *l*, *m*=1,2,3. In synthetic aperture radiometry V_{lm} is called a sample of the visibility function.

For a point source located at (ξ',η') with brightness temperature T_0 ($T_B(\xi,\eta)=T_0\cdot\delta(\xi-\xi',\eta-\eta')$), V_{lm} is given by the Van Cittert-Zernike Theorem [2, 3, 4, 5]:

$$V_{lm}=\frac{1}{2}\left\langle b_l(t-\tau_l)\ b_m^*(t-\tau_m)\right\rangle = \frac{1}{\sqrt{\Omega_l\Omega_m}}\frac{T_0}{\sqrt{1-\xi'^2-\eta'^2}}F_{n_l}(\xi',\eta')F_{n_m}^*(\xi',\eta') \tilde{r}_{lm}\left(\tau_l-\tau_m-\frac{u_{lm}\xi'+v_{lm}\eta'}{f_0}\right)\exp\left[j2\pi f_0\left(\tau_l-\tau_m-\frac{u_{lm}\xi'+v_{lm}\eta'}{f_0}\right)\right], \quad (4)$$

where Ω_l and $F_{nl}(\xi,\eta)$ are the antenna equivalent solid angle and normalized radiation voltage pattern of element *l*, $\sqrt{1-\xi'^2-\eta'^2}$ is the obliquity factor (cosine of the angle from the boresight direction), and $\tilde{r}_{lm}(t)=1/\sqrt{B_lB_m}\cdot\int_0^\infty H_{n_l}(f)H_{n_m}^*(f)\exp(-j2\pi f_0 t)\,df$ is the fringe washing function that accounts for spatial decorrelation effects, and depends on the receiver *l* and *m* normalized frequency responses $H_{n_l}(f)$ and $H_{n_m}(f)$.

If all receivers have the same normalized antenna radiation voltage pattern ($F_n(\xi,\eta)$), equivalent solid angle (Ω), and normalized frequency response, modeled by a Gaussian filter $H_n(f)=\exp\left(-\pi(f-f_0)^2/(2B^2)\right)$ centered at $f=f_0$ with equivalent noise bandwidth *B*, then $\tilde{r}_{lm}(\tau)$ becomes $\tilde{r}(t)=\exp(-\pi B^2t^2)$, and system's output for a point source the impulse response is given by:

$$V_{123}(\tau_2,\tau_3)=2\left[\frac{1}{\Omega}\frac{T_0}{\sqrt{1-\xi'^2-\eta'^2}}|F_n(\xi',\eta')|^2\right]^3\exp\left\{-\pi W^2u^2(\xi-\xi')^2\right\}\cdot \cdot\exp\left\{-\pi W^2\left[-\frac{u(\xi-\xi')}{2}+v(\eta-\eta')\right]^2\right\}\exp\left\{-\pi W^2\left[\frac{u(\xi-\xi')}{2}+v(\eta-\eta')\right]^2\right\}= =2\left[\frac{1}{\Omega}\frac{T_0}{\sqrt{1-\xi'^2-\eta'^2}}|F_n(\xi',\eta')|^2\right]^3\exp\left\{-\pi W^2\left[\frac{3}{2}u^2(\xi-\xi')^2+2v^2(\eta-\eta')^2\right]\right\}, \quad (5)$$

where $W\triangleq B/f_0$ is the relative bandwidth. If $v=\sqrt{3}/2\cdot u$, the array is an equilateral triangle with side *u*, and the impulse response ($T_0=1$) becomes a circularly-symmetric two-dimensional Gaussian function with 1/*e* widths $\sigma_\xi=\sigma_\eta=1/(\sqrt{\pi}\,W\,u)$, or half-power beamwidths $\Delta\xi_{-3\mathrm{dB}}=\Delta\eta_{-3\mathrm{dB}}=2\sqrt{2\ln 2}/\sqrt{\pi}\,W\cdot u\approx 1.3/W\cdot u$.

II. Instrument And Field Experiment DescriptionIn order to test the concept, an L-band three antenna instrument demonstrator has been built and tested. The instrument has a bandwidth of 8 MHz centered at 1413.5 MHz, and the in-phase and quadrature components of each receiver are downconverted and synchronously sampled at 1 bit and 18.357 MHz. In addition, two of the three in-phase signals are compared with a non-zero threshold for amplitude calibration purposes. Data is stored at a sustained rate of 18.357 Mbytes/s during more than 50 minutes per disk in low cost high capacity removable ATA/133 disks (Fig. 1).

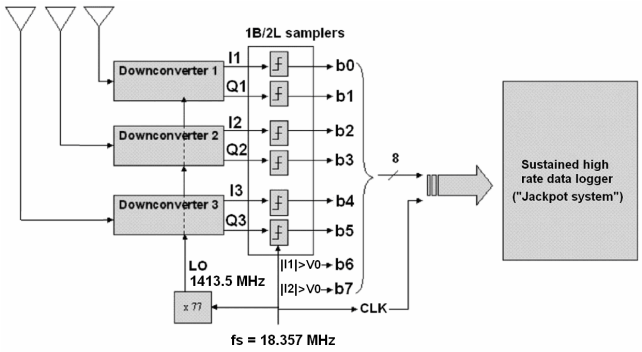

Fig. 1. Block diagram of the radiometer: 3 antennas point to the sky

Signals' cross-correlations are then computed a posteriori by software for increased flexibility. The instrument block diagram is the same as the GPS Doppler-Delay Receiver described in [6], with the same data logger, but with the following differences:

- the RF and IF filters, and the LO generation were modified to be centered in the band 1400-1427 MHz reserved for passive remote sensing, and
- due to the large antenna separation, the LO is distributed at an intermediate frequency of 128.5MHz, and the analog I/Q signals transmitted to the data logger at baseband.

Figure 2 shows one of the three L-band receivers and the data acquisition and data logger system.

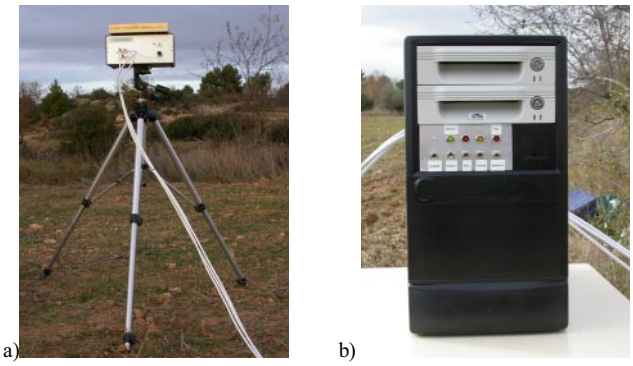

Fig. 2. a) One of the three elements mounted on top of a tripod and b) data acquisition system during the field experiment at l'Albi (Lleida, Spain, December 18, 2002).

In December 18, 2002 the array was deployed in a field at L'Albi (Lleida, Spain) forming a triangle of approximately 170 m side (Fig. 3). The antenna positions in UTM format (fuse 31), European datum, were R_1 = (0326539, 4586746, 515) , R_2 =(0326607, 4586900, 518) , and R_3=(0326702, 4586760,523) meters. Due to terrain slope, receivers' heights could not be completely equalized, which had to be taken into account during the data processing. Due to the large antenna separation, the most obvious moving natural source that could be imaged with this radiometer was the Sun. Data acquisition periods started at o'clock hours and 10 minutes (first one at 11:10 am local time), and were 10 minutes long, a compromise between the amount of data to be recorded and processed, and the movement of the Sun. Finally, the data acquisition system was located at the center of the triangle (Fig. 3).

Fig. 3 Test setup overview: Antenna 1 (red circle) and data logger (yellow circle). Cables connecting the antennas and the data logger are 100 m long and are 120º apart.

III. Data Processing And Field Experiment DescriptionA total of 105 Gbytes of data were recorded in 420 files of 256 Mbytes each. Due to computation time limitations, only the first 2^{20} samples (i.e. 57 ms of acquisition time at 18.35714 Msamples/s) of each file were processed. The data processing consisted of the computation of eqn. 3 from the normalized visibility samples ($\mu_{lm} = V_{lm} \Big/ \sqrt{T_{sys,l} T_{sys,m}}$), because of the 1 bit quantization scheme. Figure 4 shows the shape and time evolution of the raw cross-correlation function $\mu_{lm} = \overline{\text{sign}\left[b_l\left(t-\tau_l\right)\right]\text{sign}\left[b_m^*\left(t-\tau_m\right)\right]}$. It can be seen that the peak position varies with time and it is different from one baseline to the rest. If the Sun were the only (point) source, these plots should look like the fringe-washing function.

Figure 5 shows Fig. 4 plots when the time delay is translated into the (ξ,η) director cosines domain, taking into account the array geometry. The image formation process is obtained from eqn. 3, as the cubic root of the product (pixel by pixel) of the three plots in Fig. 4 multiplied by two (Fig. 5).

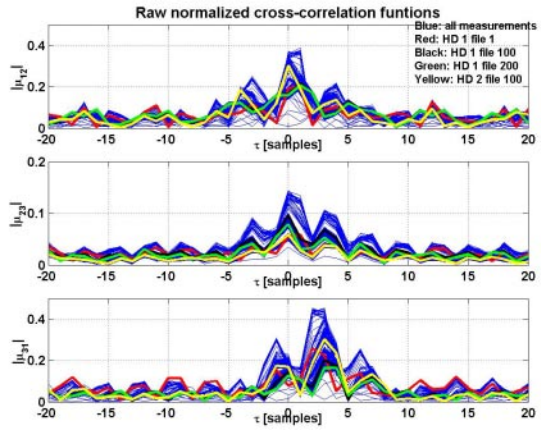

Fig. 4. Raw normalized cross-correlation functions for each antenna pair and different hard disk files. In blue, all cross-correlations have been plotted. Offset corrected, instrumental differential delays not compensated.

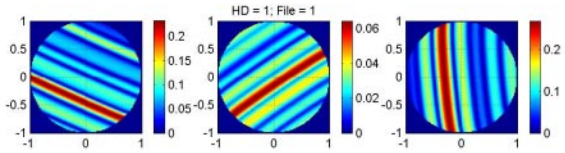

Fig. 5. Normalized responses for each antenna pair (first file, first acxquisition of L'Albi experiment). From left to right: $|\mu_{12}|$, $|\mu_{23}|$ and $|\mu_{31}|$.

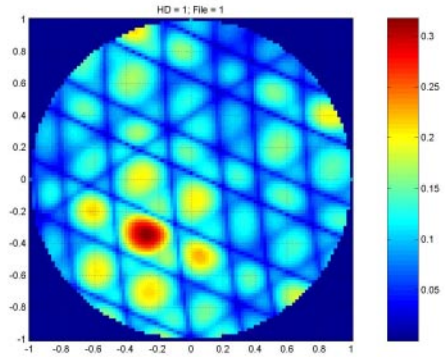

Fig. 6. Global system's response
(first file, first acquisition of L'Albi experiment).

The hottest spot is coincident with the Sun position, and the six warm spots around it are the side lobes, coming from the side-lobes of the fringe-washing function, which looks more like as a sinc function than a Gaussian function. Amplitude calibration has not been performed, but it could from the measurement of the relative number of counts of the input signal being higher than a given threshold [7].

Finally, Fig. 7 shows the global system's response for the first file of the second acquisition, one hour later. It can be seen that the peak position has moved by an amount that corresponds exactly to the movement of the Sun and, in addition, there is a small increase of the peak amplitude (closer to noon, Solar time).

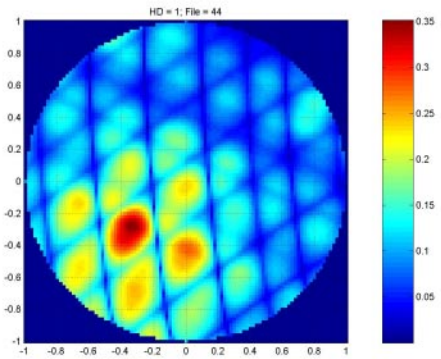

Fig. 6. Global system's response (first file, second acquisition of L'Albi experiment). As compared to Fig. 5, the shape of the systems's reponse degrades by an unknown reason.

III. Conclusions

This paper has briefly described the principles, hardware implementation, field experiment and data processing results of a new type of synthetic aperture radiometer that uses the time delay to focus pixels in the field of view. It can be considered as a first step to achieve Doppler-radiometer processing, which will enhance the angular resolution by a factor of $1/W$. Future activities include:

- improved data processing algorithms to reduce the level of side lobes, and
- controlled experiments in anechoic chamber with moving point sources so as to be able to test the full capabilities of the Doppler-processing with commensurable data processing.

Acknowledgements

This work has been performed under grant of the *Distinció de la Generalitat de Catalunya per a la Promoció de la Recerca Universitària*, 3rd edition (RESOLUCIÓ UNI/2120/2002, July 19, 2002; DOGC núm. 3684 - 24/07/2002).

References

[1] A. Camps and C.T. Swift, "2D Doppler-radiometers for Earth Observation", IEEE Transactions on Geoscience and Remote Sensing, Vol. 39, No 4, pp. 1566-1572, July 2001.
[2] Goodman, J.W. (1968). Introduction to Fourier Optics. McGraw-Hill 1968.
[3] Goodman, J.W. (1985). Statistical Optics, Wiley Interscience.
[4] Thompson, A.R.; Moran, J.M.; Swenson, G.W. (1986). Interferometry and Synthesis in Radio Astronomy. John Wiley and Sons.
[5] Camps, A. (1996). Application of Interferometric Radiometry to Earth Observation, pp. 17-30. Ph. D. dissertation, Universitat Politècnica de Catalunya.
[6] Nogués, O., A. Sumpsi, A. Camps, and A. Rius, "A 3 GPS-Channels Doppler-Delay Receiver for Remote Sensing Applications", Proceedings of the IGARSS, Toulouse, France, July 2003 (this CD-ROM).
[7] Martín-Neira, M., P. Piironen, A. Camps, L. Sempere, "Digital rms-voltage detector", Patent solicitude number: ESA/PAT/471, country France, date: August/2001.